

Prospects of nuclear physics research using rare isotope beams at RAON in Korea*

Byungsik Hong[†]

Department of Physics, Korea University, Seoul 136-701, Republic of Korea

(Received January 2, 2015; accepted in revised form March 3, 2015; published online April 20, 2015)

Korea plans to build a new radioactive ion-beam accelerator RAON together with various experimental facilities. In particular, KOBRA (the Korea Broad Acceptance Recoil Spectrometer & Apparatus) and LAMPS (the Large-Acceptance Multi-Purpose Spectrometer) will be constructed for the nuclear physics experiments. The primary goal of KOBRA is to study the structure of exotic nuclei near drip lines and various astrophysical processes at low energies. On the other hand, LAMPS will investigate the density dependence of the nuclear symmetry energy in wide beam energy range up to 2 times normal nuclear densities. This paper provides an overview of RAON and the experimental setup for the nuclear physics program.

Keywords: RAON, KOBRA, LAMPS, Radioactive ion beam, Heavy-ion collision, Drip line, Nuclear symmetry energy

DOI: [10.13538/j.1001-8042/nst.26.S20505](https://doi.org/10.13538/j.1001-8042/nst.26.S20505)

I. INTRODUCTION

A radioactive ion-beam (RIB) accelerator is an essential machine to study various properties of nuclei and nuclear matter with unusual neutron-to-proton ratios (N/Z). Interesting topics relevant to the heavy-ion collisions with RIB include the origin of the heavy elements, the astrophysical processes in stars, the nuclear structure near drip lines, and the nuclear symmetry energy.

The new generation RIB accelerators extend our understanding of the modified nuclear structure with extraordinary N/Z and their reactions with unprecedented precision. New accelerators provide users more exotic RIBs with much higher intensity than previously achieved [1]. Korea also launched the new project for the construction of a forefront radioactive ion-beam accelerator and various experimental facilities in 2011. In order to lead the construction project, RISP (the rare isotope science project) was set up at the newly established Institute for Basic Science (IBS) in Korea. The primary goal of RISP is to design and complete the new RIB accelerator RAON, which is a pure Korean word meaning ‘delightful’, and experimental devices not only for basic sciences but also for various applications. In the future, RAON is expected to provide new opportunities to researchers working, in particular, for the nuclear physics using RIB.

In following, the paper summarizes the design and the current status of RAON and the two spectrometers for nuclear physics, KOBRA and LAMPS. Section II introduces the conceptual design of the RAON accelerator. Sections III and IV describe the recoil spectrometer KOBRA and the large-acceptance spectrometer LAMPS, respectively. The current status of the development for the time-projection chamber (TPC) and the neutron detector array for LAMPS are also briefly given in Section IV. The paper ends with a summary in Section V.

II. RAON: A NEW RIB ACCELERATOR

Figure 1 shows a schematic diagram of the RAON accelerator facility [2, 3]. The special feature of the RAON facility is the combination of the two different RIB production methods, namely the in-flight fragmentation (IF) and the isotope separator on-line (ISOL). The specifications of the beams for the driver linear accelerator (LINAC), the post accelerator, and the cyclotron are summarized in the table in Fig. 1.

The RAON’s ISOL system is driven by a high current cyclotron that provides 1 mA proton beams at a beam energy of 70 MeV. Radioactive isotopes in the ISOL system are generated in the direct fission of ^{238}U target. Preventing over heated, the low-density ($2.5\sim 5 \text{ g/cm}^3$) porous UC_x target is to be prepared in a thin multi-disk shape. A post accelerator (SCL3) after the target increases the beam energy up to 18.5 MeV/u for users in the low energy experimental hall.

The RAON’s IF system produces radioactive isotopes by fragmentating ^{238}U or other heavy beams. The charge state of U beam for SCL1 is either +33 or +34 with an average of +33.5. In the superconducting driver LINAC system SCL2, the charge state will be distributed from +77 to +81 with an average of +79 after the charge stripper section. The U^{+79} projectile can be accelerated up to 200 MeV/u at the end of SCL2.

The IF separator, as shown in Fig. 2, consists of pre- and main separators and the matching section in between them [4]. The primary beam particles bombard the production target at the focal plane F0 for the projectile fragmentation. The selection of the desired radioactive ion beams occurs in the pre-separator part. The unwanted primary beam particles stop at the dispersive focal plane F1 by a beam dump. After the double achromatic focal plane F2, the beam particles pass the wedge-shape degrader at dispersive focal plane F3. The dispersion matching can be done in between the two achromatic foci F4 and F5, although the exact location of this section is still under discussion. The selected beam particles after the matching section are either introduced to the main separator or delivered to the large-acceptance spectrometer. When the selected beams are introduced to the main separator, they impinge the experimental target at the dispersive

* Supported by the National Research Foundation of Korea (Nos. 2012M7A1A2055596 and 2013M7A1A1075898)

† Corresponding author, bhong@korea.ac.kr

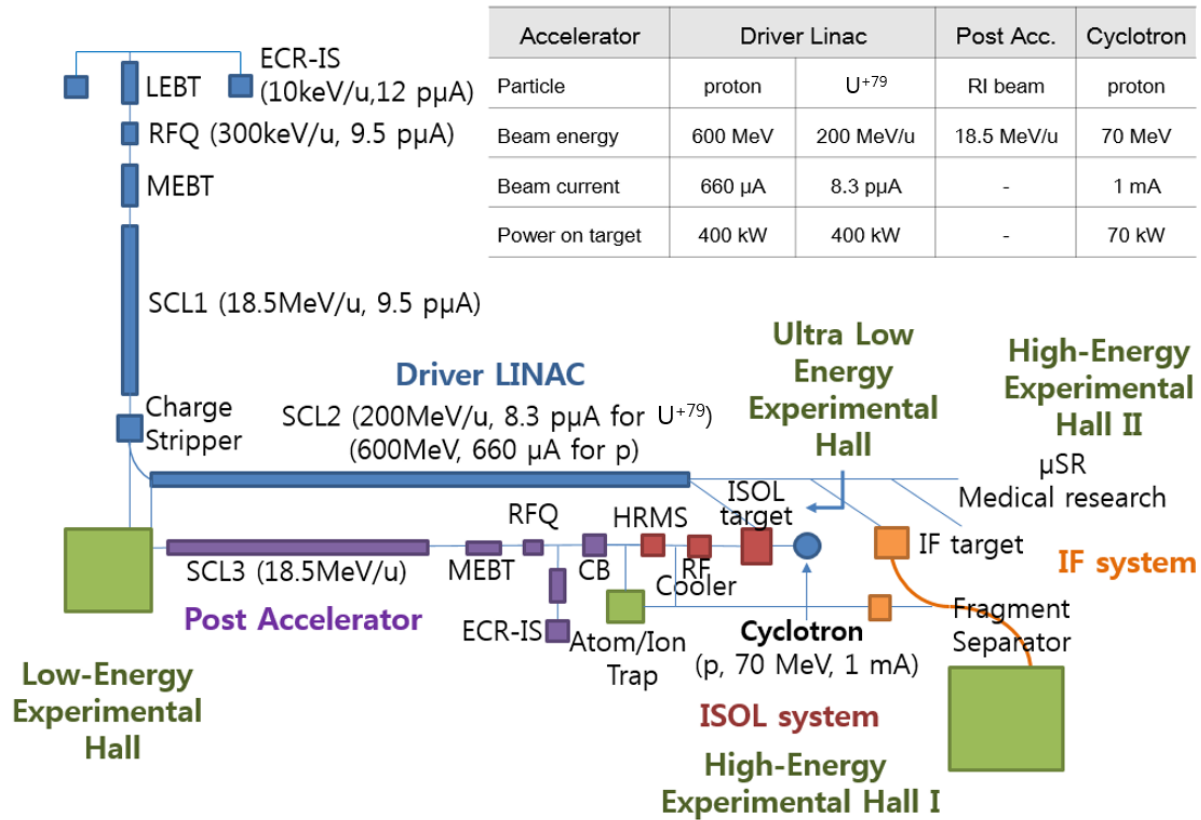


Fig. 1. (Color online) Schematic diagram of the planned RAON facility [2, 3]. The acronyms are defined as follows: ECR-IS (electron cyclotron resonance ion source), RFQ (radio frequency quadrupole), LEBT (low energy beam transport), MEBT (medium energy beam transport), SCL (superconducting linear accelerator), HRMS (high resolution mass separator), and CB (charge breeder). Beam specifications of the driver LINAC, the post accelerator, and the cyclotron of the RAON facility are summarized in the upper-right table. Note that the number of charge state (+79) for U beam is the average value. See text for the details. Figure was adopted from [3] and modified.

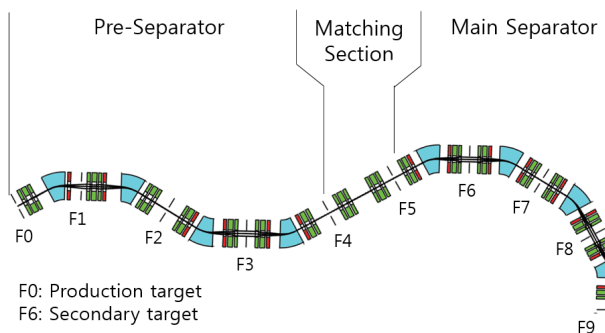


Fig. 2. (Color online) Schematic diagram of the IF separator for RAON [4].

focal plane F6. Then, the secondary projectile fragments are further selected and transferred to the detector system. For particle identification at the main separator, each focal point is equipped with PPAC (parallel plate avalanche chamber), the plastic scintillator detector and the slit system.

In the current design of the RAON's IF system, the momentum acceptance is $\pm 4.3\%$. The horizontal and vertical

angular acceptances are ± 40 and ± 50 mrad, respectively. It is being discussed to increase the aperture of the superconducting quadrupole magnets from the current 34 cm to 36 cm in order to enhance the momentum acceptance up to $\pm 5\%$ [4]. The maximum magnetic rigidity is about 10 T·m for uranium beams at 400 MeV/u, considering the future beam-energy-upgrade option. The resolving powers ($p/\Delta p$) at F1, F3, F6 and F7 are 1250, 1520, 1350 and 2100, respectively.

TABLE 1. Expected energy ranges and intensities at the experimental target for some selected radioactive ion beams at RAON.

Beam nuclide	Energy (MeV/u)	Intensity (pps)
^{106}Sn	10–250	$\sim 10^9$
^{132}Sn	5–250	$\sim 10^7$
^{140}Xe	10–250	$\sim 10^8$
^{142}Xe	10–250	$\sim 10^7$

The RAON's ISOL and IF systems can be operated independently, serving more users simultaneously. However, the unique and innovative idea of RAON is to combine the two techniques, i.e., the radioactive ion beams from the ISOL system are transferred to the driver LINAC SCL2 and bombard the in-flight target for more exotic RIBs at high energies. This

TABLE 2. Setups being conceived at each experimental halls at RAON.

Experimental hall	Conceivable setups	Scientific goals
Ultra low-energy hall	High-precision mass-measurement system Collinear laser spectroscopy system	Properties of exotic nuclei Fundamental symmetries
Low-energy hall	KOBRA recoil spectrometer Low-energy LAMPS β -NMR system Neutron science facility Bio-medical science facility	Properties of exotic nuclei Nuclear symmetry energy Condensed matter physics Nuclear data measurement Bio and medical researches
High-energy hall-I	High-energy LAMPS Zero-degree spectrometer	Nuclear symmetry energy Properties of exotic nuclei
High-energy hall-II	μ SR system Bio-medical science facility	Condensed matter physics Bio and medical researches

combination has strong potential to yield more exotic radioactive ion beams that cannot be achieved by either ISOL or IF alone. According to the LISE++ calculations, the intensity of the exotic nuclei in the combination mode are about a factor of 1000 higher than those achieved by the IF system alone. A combination of ISOL and IF systems is expected to broaden the nuclear landscape for the forefront nuclear physics research at RAON. Some representative beams that will be available at RAON are summarized in Table 1 with beam energy ranges and intensities.

According to the current plan, RAON will provide four experimental halls for users. The conceivable experimental setups for each experimental hall are summarized in Table 2 along with the relevant sciences. The scientific goal of RAON is broad, covering from the fundamental physics to various applications. Nevertheless the most important research field of RAON is the nuclear physics. The relevant experimental halls for nuclear physics are the low-energy hall and the high-energy hall-I, where the KOBRA and LAMPS systems are planned to be located. In the following sections, the current design and the physics goals of the two experimental setups are described.

III. KOBRA: A RECOIL SPECTROMETER

Figure 3 displays the design of the KOBRA recoil spectrometer, which consists of an upstream in-flight separator and a downstream big-bite spectrometer. The KOBRA recoil spectrometer is for nuclear structure and nuclear astrophysics at beam energies up to 18.5 MeV/u. The in-flight separator consists of two dipole magnets (D1 and D2) and a Wien filter (W1), and the big-bite spectrometer consists of a dipole magnet (D3) and another Wien filter (W2). In Fig. 3, F0, F2, F3 and F4 are achromatic focal planes, and F1 and F5 are dispersive focal planes. In the current design, the momentum acceptance is $\pm 7\%$, and the horizontal and vertical angular acceptances are ± 20 and ± 100 mrad, respectively. The maximum magnetic rigidity is about 2 T·m with the resolving power of momentum being better than 0.5%. The background reduction factor is expected to be at least 10^{-12} with the current design.

Two operational modes are available for KOBRA. The first

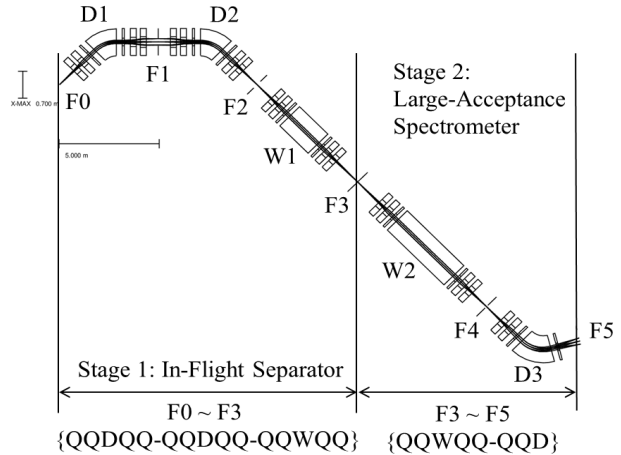


Fig. 3. Recoil spectrometer KOBRA at RAON. Adopted from [3].

possibility is the IF mode, where the stable ion beams generated by one of the two ECR ion sources are accelerated and impinge the production target at F0. Then, the selected secondary radioactive ion beams are delivered to the experimental target at F3. The second possibility is the ISOL mode, where the radioactive ion beams generated by the ISOL system are accelerated and delivered to the experimental target at F3 so that the first stage of KOBRA further purifies the beams. In both cases, all detection systems are located at F3. Presently, for example, the gas-jet target, the Si array and the gamma array are being developed.

The physics program of KOBRA is focused on the structure of exotic nuclei near the drip lines, the discovery of rare events including new isotopes and superheavy elements, and the various astrophysical reactions related to the r - and rp -processes. A total of about 10 000 isotopes are theoretically predicted, but only about 3000 stable and unstable isotopes are experimentally found so far. As a result, it will be highly important for RAON to discover the exotic nuclei, especially, near the neutron drip line for completing the nuclear chart and understanding the limit of existence for nuclei. Another example in nuclear astrophysics is the capture reaction $^{15}\text{O}(\alpha, \gamma)^{19}\text{Ne}$, which links the CNO (or hot-CNO) cycle and the rp -process, as explained in Fig. 4.

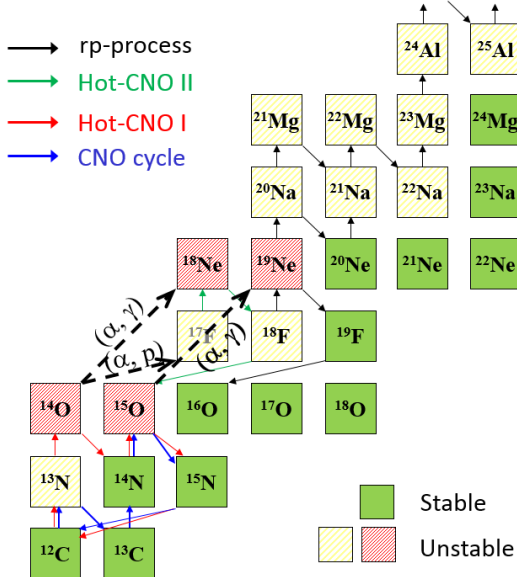


Fig. 4. (Color online) Part of the nuclear chart, explaining the importance of the capture reactions in nuclear astrophysics. The dashed arrows represent the breakout reactions from the CNO (or hot-CNO) cycle to the rp-process.

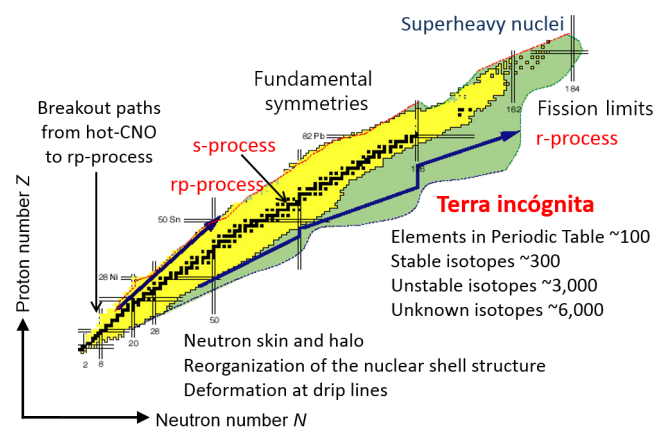


Fig. 5. (Color online) Nuclear chart with some interesting research topics that can be explored at KOBRA in the future. The black squares display the stable isotopes and the yellow band represents the unstable isotopes discovered in the laboratory. The dark green area, also called as ‘Terra incógnita’, represents the region for the theoretically predicted, but not yet discovered isotopes.

The experimental observables for these studies are the cross sections, the decays, the transfer reactions, the radiative capture reactions, the fusion evaporation processes, and elastic & inelastic scatterings. Thanks to its excellent capability for tagging and separation of the recoiled nuclei, KOBRA will be a powerful device for studying them. Fig. 5 summarizes some interesting research topics, which can be explored at KOBRA, on the nuclear chart.

IV. LAMPS: LARGE-ACCEPTANCE DETECTOR SYSTEMS

The primary goal of LAMPS is to investigate the nuclear symmetry energy which is essentially the difference between the energy per nucleon of pure neutron matter and that of isospin symmetric matter [5]. The nuclear symmetry energy can be expanded in series (usually up to second order) as a function of the baryon density around the saturation value ρ_0 . Then, the coefficients of the first (slope) and the second term (curvature) reflect the symmetry pressure and the compressibility, respectively, of nuclear matter. Although some experimental data is available for the nuclear symmetry energy around ρ_0 , the detailed information for dense matter are still missing. Therefore, LAMPS plans to build two detector systems, one for low-energy beams up to 18.5 MeV/u and another for high-energy beams up to about 250 MeV/u, to study the density dependence of the nuclear symmetry energy up to about 2 – 3 times ρ_0 .

The symmetry energy is important to understand the many-body theory of strongly interacting systems as well as various astrophysical objects, such as the core of the neutron stars [6]. The radioactive ion-beam accelerators are essential for the detailed study of the nuclear symmetry energy since they can provide nuclear matter with extraordinary N/Z in sub- and supra-saturation densities. As a result, RAON and the experimental setups are expected to play an important role in future symmetry-energy studies as it provides high-intensity RIBs with a broad beam energy range [3].

A. LAMPS-L: Low-energy LAMPS

To study the nuclear symmetry energy at sub-saturation densities, RAON plans to build the low-energy LAMPS (LAMPS-L) at the low-energy experimental hall. LAMPS-L consists of a spherical Si-CsI system and a neutron detector array [3]. A Si-CsI system surrounds the experimental target, and measures the charged particles and γ 's with an energy resolution ($\Delta E/E$) of about 1% at large angles. A neutron detector array is located in forward angles, and measures the kinetic energy of neutrons with $\Delta E/E$ better than 5% via the time of flight.

Since the identification of the beam residue is essential, especially, for the dipole γ emission in the nuclear-symmetry-energy study, LAMPS-L is desired to be positioned at the focal plane F3 of the KOBRA recoil spectrometer. In order to fit into the space available between the first and the second stages of KOBRA, the LAMPS-L setup must be compact, and the distance from the target to the neutron detector array needs to be less than about 2 m. The current LAMPS-L design enables us to estimate the excitation energy of the reaction by kinematically complete measurement of all emitted particles.

Figure 6 shows the design of the LAMPS-L system for the study of nuclear symmetry energy. The Si-CsI system consists of ~93 detector modules, spanning the laboratory polar angle θ_{lab} from 17.5° to 145°. Each module is composed

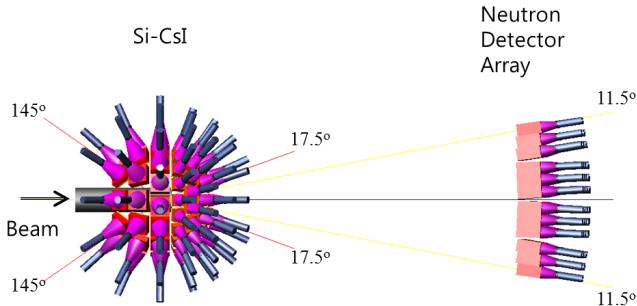


Fig. 6. (Color online) Schematic design of the LAMPS-L system at F3 of the KOBRA recoil spectrometer at RAON. Adopted from Ref. [3].

of a Si-strip (or pixel) layer and a rectangular-parallelepiped CsI(Tl) block. The active cross-sectional area of the unit module is smaller in the forward direction than in large angles to handle the $\theta_{1\text{ab}}$ -dependent multiplicity: 9 cm×9 cm in $17.5^\circ < \theta_{1\text{ab}} < 77.5^\circ$ and 15 cm×15 cm in $77.5^\circ < \theta_{1\text{ab}} < 145^\circ$. The occupancy with this configuration is estimated to be lower than 15% for head-on $^{132}\text{Sn} + ^{124}\text{Sn}$ collisions for the PHITS generator at 18.5 MeV/u [7]. Each silicon strip (or pixel) layer is 100 μm thick and the CsI(Tl) block is 5 cm deep. At 20 MeV the photo-peak efficiency of the CsI(Tl) block is higher than 30% with threshold of 1 MeV.

The neutron detector array consists of a total of 120 modules. The signal from a plastic scintillator block is read out by a photomultiplier tube (PMT). To obtain the maximal light yield, the shape of light guide is optimized. The cross-sectional area of each scintillator block is 10 cm×10 cm and the depth is 20 cm. The simulation by GEANT4 [8] demonstrates that the neutron efficiency is about 40% with a threshold of 1 MeV. Assuming that the time resolution is 500 ps, the energy resolution for neutrons is expected to be about 3.3% at 10 MeV.

One of the prominent observables for the nuclear symmetry energy at low energies is the dipole γ emission in fusion reactions. The recent model calculations have shown that the collective dipole bremsstrahlung radiation is expected during the fusion process between two nuclei at about 180 MeV/u [9, 10]. The microscopic transport models predict that the γ strength is larger for softer nuclear symmetry energy. In addition, the current experimental results show that the γ strength increases with the isospin asymmetry of the collision system albeit huge error bars [11]. Therefore, it is necessary for the future RIB experiments to provide precise and systematic results, especially, with the large N/Z collision systems.

B. LAMPS-H: High-energy LAMPS

The most important purpose of the LAMPS-H system is to measure various observables simultaneously for the nuclear symmetry energy above the saturation density. Fig. 7 shows the LAMPS-H system that is a combination of a

solenoid spectrometer and a dipole spectrometer with a forward neutron-detector array. The density of the generated nuclear matter can be controlled by the collision centrality and the beam energy. Various charged particles, including pions and fragments, are planned to be measured in a large geometrical acceptance ($> 3\pi$) by a solenoid spectrometer. The beam residue and neutrons are measured by a dipole spectrometer and the neutron array, respectively, in the forward region. The current design of LAMPS-H allows comprehensive analysis of the various promising observables, such as the yield ratio of the isospin mirror nuclei, the π^-/π^+ ratio, the direct and elliptic flows, and the isospin diffusion, for the nuclear symmetry energy. The following subsections describe the design and the current R&D status of the time-projection chamber (TPC) and the neutron array. Note that the Si-CsI detector, covering $14^\circ < \theta_{1\text{ab}} < 24^\circ$, for LAMPS-H measures the charged particle distributions in forward angles beyond the TPC acceptance. This information will be also useful to determine the collision centrality and the reaction plane of each event.

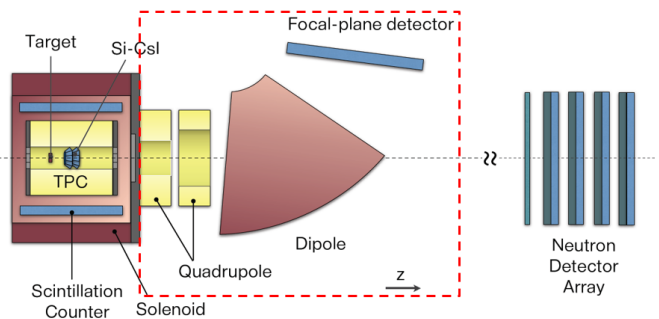


Fig. 7. (Color online) Schematic design of the LAMPS-H system at RAON. Adopted from Ref. [3] and modified.

1. TPC: Time-projection chamber

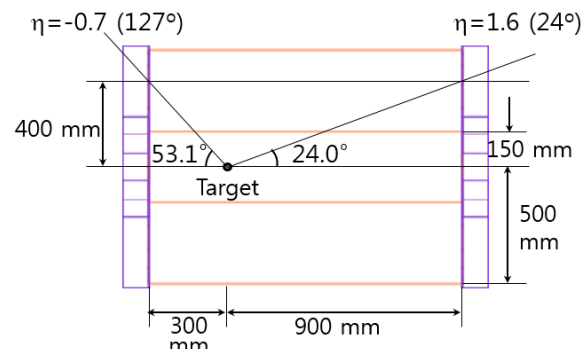


Fig. 8. (Color online) Structure and dimensions of the LAMPS-H TPC.

The heart of the LAMPS-H solenoid spectrometer is the TPC. A TPC is a 3-dimensional tracking device utilizing the drift of ionized electrons in a gas mixture [12]. Fig. 8 shows

the geometry and dimensions of the LAMPS-H TPC which covers θ_{lab} from 24° to 127° . For the gas vessel, the length along the beam axis is 1.2 m, and the inner and outer radii are 15 and 50 cm, respectively. A high-voltage membrane is positioned in the middle of the gas vessel, which drifts the ionized electrons to the readout device as the electric and magnetic fields are parallel. The target is nominally placed at 30 cm from the upstream edge of the vessel.

The GEM (the gas-electron multiplier) will be used for signal readout of the TPC [13]. A triple GEM (a GEM detector with three GEM foils) is installed at each end of the TPC. Each triple GEM detector consists of the eight identical octants azimuthally. The GEM foil is made of $50\text{ }\mu\text{m}$ thick kapton foil sandwiched by two $5\text{ }\mu\text{m}$ thick copper layers. The radius of each GEM hole is about $35\text{ }\mu\text{m}$ with a pitch of $57.5\text{ }\mu\text{m}$.

The TPC characteristics have been extensively simulated by using GARFIELD++ [14]. Each GEM foil is biased at 450 V, and the gas vessel is filled with C10 (90% Ar + 10% CO₂). The simulation has returned that the mean of the gain distribution for a triple GEM is about 1.4×10^6 and that the transversal spread of electrons after drifting 60 cm is about 3 mm. Note that the transversal spread for C10 is about 25% smaller than that obtained for another popular gas mixture P10 (90% Ar + 10% CH₄). The drift velocity of the ionized electrons with C10 is $\sim 50\text{ mm/us}$, which is about a factor of two larger than that obtained with P10.

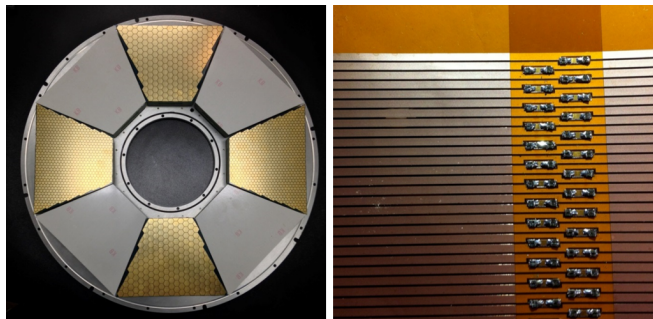


Fig. 9. (Color online) Pictures of the pad plane (left) and the electric-field plane (right) of the prototype TPC for LAMPS-H.

The LAMPS group has designed and built the prototype TPC to understand the detailed performance. The dimensions of the prototype TPC are about 1/2 of those of the real size: its length and outer radius are 57 cm and 24.5 cm, respectively. The triple GEM and the readout pad plane are placed on one end and the high-voltage cathode plane is placed on another end of the gas vessel. The shape of each readout pad is hexagonal with 2.5 mm or 5 mm long sides. For the present prototype, the TPC has only four out of eight octant sectors completed, as shown in the left panel of Fig. 9. The side dimensions for each hexagonal pad is 2.5 mm for the two sectors and 5 mm for the other two sectors, which allows us to compare the performance between them. The right panel of Fig. 9 is the picture of the field plane composed of Cu strips (2 mm wide) on the kapton foil (35 μm thick). The mirror strips are also placed on the back side of the kapton foil and



Fig. 10. (Color online) Pictures of the prototype TPC after the outer field cage is installed (left) and the assembly is completed (right). In the right-bottom corner of the right picture the prototype GET electronics board can be found.

a $1\text{ M}\Omega$ resistor is connected to each Cu strip. The cylinder body of gas vessel for the prototype TPC is constructed with layers of the field plane, G10 and honeycomb panel. The left picture of Fig. 10 shows the prototype TPC after the outer field cage is installed, and the right picture shows the one after the assembly was completed.

According to the simulation, more than a million avalanche electrons are expected in each 2.5 mm pad and the gain should be high enough for signal processing. If the side dimensions of each pad are 2.5 (5) mm, the total pad number will be about 90 000 (20 000) for both sides. The detailed data analysis of the prototype TPC and simulations are needed to optimize the size of each pad in the future. In addition, a track reconstruction program is being actively developed.

2. Neutron detector array

The neutron detector array for LAMPS-H consists of eight layers along the beam direction. Each layer consists of twenty scintillator bars, and every two layers are paired to form a total of four stations with the gap between two stations being larger than 30 cm. The dimensions of each scintillator bar are $0.1\text{ m} \times 0.1\text{ m} \times 2.0\text{ m}$. As the long side of each bar is aligned along the vertical and horizontal directions in the first and second layers, respectively, for each station, the neutron array provides the two-dimensional hit information. A veto detector is positioned right before the neutron detector array. The dimensions of the veto detector are exactly the same as those of a single neutron-array layer except the thickness is 5 cm. The signals from each scintillator bar are read out by PMT at both ends. In order to maximize the light collection, an acrylic light guide is placed in between the scintillator bar and PMT. Two real-size prototype neutron detectors have been constructed and tested using the radiation sources to estimate the performance of the neutron array [15, 16]. The scintillation bars are made of a polyvinyltoluene-based BC-408 model from Saint-Gobain Crystals, Inc., which has a relatively fast response time with a relatively narrow pulse

width [17].

To examine the detector performance for incoming neutrons, a ^{252}Cf source is used. As shown in Fig. 11, a ^{252}Cf source is positioned at 1 m from the center of the prototype detectors and the trigger detector is placed right next to the source in order to effectively increase the acceptance and the trigger rate. The space between the source and the prototype detector is shielded by lead and paraffin bricks except for the central opening. The uncertainty of the flight pathlength with an opening of 60 cm is about 0.25 cm. Assuming 0.25 cm as the sole uncertainty and propagating it properly, the estimated systematic error on the kinetic energy of neutrons is about 0.6% [15].

Most events have one associated hit in a single prototype detector, but about 0.5% of the total events have two associated hits. In order to test a very primitive clusterization concept, two prototype detectors are stacked on top of each other. The two close hits in time with a large temporal gap from their neighbor hits form a cluster. Assuming that the hits in a cluster originated from the same incident neutron, the earlier signal is taken for the consecutive analysis. Since the number of clusters is unfortunately too small this time, a neutron peak in the mean-time distribution cannot be reconstructed. Therefore, it is desirable to use more scintillator bars for the cluster formation in the future, which helps to study the detailed position and energy dependences.

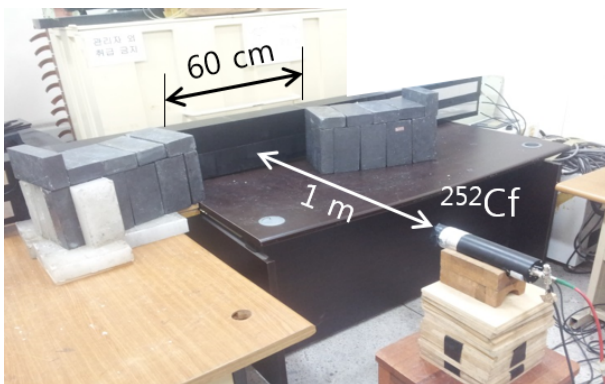


Fig. 11. (Color online) Picture of the experimental setup for the test of the prototype neutron detector using the ^{252}Cf source.

Using the experimental setup shown in Fig. 11, the scintillator bars and the trigger PMT receive not only neutrons but also γ 's. The correlation between the time and the charge shows that the slow neutrons can be clearly separated from the fast γ 's. As a result, by applying the cut to the neutrons, the mean-time distribution of neutrons from ^{252}Cf can be reconstructed. Note that the secondary events not directly from the ^{252}Cf source are subtracted statistically. The secondary events are measured by completely blocking the direct path between the source and the detector. For the current data sample, secondary events amount to $\sim 30\%$ with a similar shape to the inclusive distribution. Finally, the kinetic energy spectrum of neutrons from ^{252}Cf has been reconstructed and compared to the empirical Watt function [18, 19]. This comparison demonstrates that the present real-size prototype neutron

detector works for energy above ~ 6 MeV [15].

The neutron detector array is to be installed about 10 m from the target in the LAMPS-H system. In addition, the mean kinetic energy of neutrons from the nuclear reactions at 250 MeV/u is expected to be about 80 MeV [20], corresponding to the mean arrival time of 86 ns. Assuming that the uncertainty of the flight distance is 2.5 cm and that the uncertainty of the mean arrival time is 0.3 ns, the error of the kinetic energy for neutrons is estimated at about 1%.

3. Coulomb breakup experiments

LAMPS-H is also a suitable device to detect the E1 electric dipole emission of the excited neutron-rich isotopes, which is one of the promising observables for the nuclear symmetry energy. In the excitation energy spectra of neutron-rich Sn isotopes (^{130}Sn and ^{132}Sn) peaks around 10 MeV named the pygmy dipole resonances (PDR) were observed [21, 22]. The fractional strength of the PDR can be related to the nuclear symmetry energy and, then, the radius of the neutron distribution [22, 23]. Furthermore, the giant dipole resonance (GDR) and the giant monopole resonance (GMR) can provide the critical information on the nuclear symmetry compressibility. For E1 excitation, the spherical gamma detector array will replace the solenoid spectrometer of the LAMPS-H setup. The HPGe (high-purity germanium) detector to be built by the nuclear structure group (or the LAMPS-L Si-CsI detector) can be utilized.

The other Coulomb breakup processes can be studied by using the modified LAMPS-H setup. For example, the neutron skin and halo structures for isotopes near the neutron drip line can be pursued by detecting the projectile fragments in the dipole spectrometer and 1 or 2 neutrons in the neutron array [24]. It is also possible to study the detailed nuclear structure of the proton-rich isotopes by (γ, p) , (p, p') , $(p, 2p)$, (p, pn) processes.

V. SUMMARY

A new radioactive-ion beam accelerator RAON is planned to be built in Korea. The main focus of RAON is the fundamental research on nuclear physics. Two major detector systems, KOBRA and LAMPS, are being designed for nuclear physics at RAON. KOBRA is a broad acceptance recoil spectrometer for nuclear structure and nuclear astrophysics with radioactive-ion beams up to 18.5 MeV/u. LAMPS is a large-acceptance multipurpose spectrometer focussing on the nuclear symmetry energy. In order to study the density dependence of the nuclear symmetry energy, two LAMPS systems are being developed at low-energy as well as high-energy experimental halls. The low-energy LAMPS system covers the sub-saturation density range up to about 18.5 MeV/u, and the high-energy LAMPS system does the supra-saturation density range up to about 250 MeV/u.

KOBRA consists of an in-flight separator and a big-bite spectrometer. The in-flight separator is made of two dipole

magnets and a Wien filter, which either selects and deliver secondary beams in the IF mode or purifies the radioactive ion beams in the ISOL mode. Various detection systems, including the windowless gas-jet target, the large-acceptance Si array and the γ array, are being actively developed.

The low-energy LAMPS consists of a spherical Si-CsI system surrounding the experimental target for charged particles and γ 's and the neutron detector array in forward. Combining the low-energy LAMPS with KOBRA, it becomes a powerful system for the symmetry-energy study as the second stage of KOBRA identifies the beam fragments with high

precision. The high-energy LAMPS combines a solenoid and dipole spectrometer with the forward neutron array. In the high-energy LAMPS, the charged pions and clusters can be measured in large acceptance by the TPC and the beam fragments can be measured at forward by a dipole spectrometer.

The high-intensity radioactive ion beam facility RAON is expected to greatly advance our knowledge of the nuclear structure and the properties of nuclear matter with extraordinary isospin compositions. This information may also shed some light on many fundamental but unknown astrophysical questions, such as the nuclear reactions in supernovae and the properties of neutron stars.

- [1] Fulton B R. Present and future RIB facilities. *J Phys Conf Ser*, 2011, **312**: 052001. DOI: 10.1088/1742-6596/312/5/052001
- [2] RISP website. http://www.risp.re.kr/eng/orginfo/intro_project.do.
- [3] Hong B, Ahn J K, Go Y, *et al.* Plan for nuclear symmetry energy experiments using the LAMPS system at the RIB facility RAON in Korea. *Eur Phys J A*, 2014, **50**: 49. DOI: 10.1140/epja/i2014-14049-2
- [4] Tshoo K, Kim Y K, Kwon Y K, *et al.* Experimental systems overview of the Rare Isotope Science Project in Korea. *Nucl Instrum Meth B*, 2013, **317**: 242–247. DOI: 10.1016/j.nimb.2013.05.058
- [5] Li B A, Chen L W and Ko C M. Recent progress and new challenges in isospin physics with heavy-ion reactions. *Phys Rep*, 2008, **464**: 113–281. DOI: 10.1016/j.physrep.2008.04.005
- [6] Steiner A W, Prakash M, Lattimer J M, *et al.* Isospin asymmetry in nuclei and neutron stars. *Phys Rep*, 2005, **411**: 325–378. DOI: 10.1016/j.physrep.2005.02.004
- [7] Particle and Heavy Ion Transport code System. <http://phits.jaea.go.jp>.
- [8] GEANT4. <http://geant4.cern.ch>.
- [9] Rizzo C, Baran V, Colonna M, *et al.* Symmetry energy effects on fusion cross sections. *Phys Rev C*, 2014, **83**: 014604. DOI: 10.1103/PhysRevC.83.014604
- [10] Wu H L, Tian W D, Ma Y G, *et al.* Dynamical dipole γ radiation in heavy-ion collisions on the basis of a quantum molecular dynamics model. *Phys Rev C*, 2010, **81**: 047602. DOI: 10.1103/PhysRevC.81.047602
- [11] Klimkiewicz A, Paar N, Adrich P, *et al.* Nuclear symmetry energy and neutron skins derived from pygmy dipole resonances. *Phys Rev C*, 2007, **76**: 051603. DOI: 10.1103/PhysRevC.76.051603
- [12] Max J N and Nygren D R. The time projection chamber. *Phys Today*, 1978, **31**: 46–53. DOI: 10.1063/1.2994775
- [13] Sauli F. GEM: A new concept for electron amplification in gas detectors. *Nucl Instrum Meth A*, 1997, **386**: 531–534. DOI: 10.1016/S0168-9002(96)01172-2
- [14] Garfield++ – simulation of tracking detectors. <http://garfieldpp.web.cern.ch/garfieldpp>.
- [15] Lee K, Lee K S, Hong B, *et al.* Performance of a real-size prototype neutron detector for the LAMPS at RAON. *J Korean Phys Soc*, 2014, **65**: 610–615. DOI: 10.3938/jkps.65.610
- [16] Lee K, Lee K S, Mulilo B, *et al.* Source test of the prototype neutron detector for the large-acceptance multipurpose spectrometer at RAON. *J Korean Phys Soc*, 2013, **62**: 1227–1232. DOI: 10.3938/jkps.62.1227
- [17] Saint-Gobain crystals. <http://www.detectors.saint-gobain.com>.
- [18] Watt B. Energy spectrum of neutrons from thermal fission of U^{235} . *Phys Rev*, 1952, **87**: 1037–1041. DOI: 10.1103/PhysRev.87.1037
- [19] Smith A B, Fields P R and Roberts J H. Spontaneous fission neutron spectrum of Cf^{252} . *Phys Rev*, 1957, **108**: 411–413. DOI: 10.1103/PhysRev.108.411
- [20] Reisdorf W, Best D, Gobbi A, *et al.* Central collisions of Au on Au at 150, 250 and 400 A-MeV. *Nucl Phys A*, 1997, **612**: 493–556. DOI: 10.1016/S0375-9474(96)00388-0
- [21] Adrich P, Klimkiewicz A, Fallot M, *et al.* Evidence for pygmy and giant dipole resonances in ^{130}Sn and ^{132}Sn . *Phys Rev Lett*, 2005, **95**: 132501. DOI: 10.1103/PhysRevLett.95.132501
- [22] Tao C, Ma Y G, Zhang G, *et al.* Symmetry energy dependence of the pygmy and giant dipole resonances in an isospin dependent quantum molecular dynamics model. *Nucl Sci Tech*, 2013, **24**: 030502.
- [23] Carbone A, Colo G, Bracco A, *et al.* Constraints on the symmetry energy and neutron skins from pygmy resonances in ^{68}Ni and ^{132}Sn . *Phys Rev C*, 2010, **81**: 041301. DOI: 10.1103/PhysRevC.81.041301
- [24] Tanaka K, Yamaguchi T, Suzuki T, *et al.* Observation of a large reaction cross section in the drip-line nucleus ^{22}C . *Phys Rev Lett*, 2010, **104**: 062701. DOI: 10.1103/PhysRevLett.104.062701